

# Archival observations of the ultra-soft X-ray transient 4U 1630-47

A.N. Parmar<sup>1</sup>, O.R. Williams<sup>1</sup>, E. Kuulkers<sup>1</sup>, L. Angelini<sup>2\*</sup>, and N.E. White<sup>2</sup>

<sup>1</sup> Astrophysics Division, Space Science Department of ESA, 2200 AG Noordwijk, The Netherlands

<sup>2</sup> Laboratory for High Energy Astrophysics, NASA Goddard Space Flight Center, Greenbelt, MD 20771, USA

Received 28 May 1996 / Accepted 17 July 1996

**Abstract.** We report on archival observations of the *ultra-soft* X-ray transient 4U 1630–47. In 1979 February, 1989 March, and 1994 September, 4U 1630–47 was observed in outburst by the *Einstein* High Resolution Imager (HRI), the *Ginga* Large Area Counter (LAC) and the *ASCA* Gas Imaging Spectrometers, respectively. In 1987 October, the *Ginga* LAC observed the region of sky containing 4U 1630–47 and a faint source was detected. While it is possible that this emission originates from another object within the LAC field of view, its properties are consistent with an observation towards the end of an outburst. The times of the *Ginga* outbursts are consistent with the known  $\sim 600$  day ephemeris. However, the *ASCA* observation and observations of the subsequent outburst by the *Rossi* X-ray Timing Explorer, indicate that these outbursts started 100–150 days later than predicted. This delay confirms the occurrence of more complex outburst behavior from 4U 1630–47.

Finally, an observation by the imaging *Einstein* HRI in 1980 February, approximately mid-way between expected outburst times, revealed a faint source at a position consistent with 4U 1630–47. The measured source intensity is higher than the previous best upper-limit. This implies that (a) the quiescent intensity is variable by a factor  $\sim 10$ , or (b) that the 1979 outburst had an extremely long duration, or (c) that the emission originates from previously undetected inter-outburst activity.

**Key words:** accretion – binaries: close – stars: individual(4U 1630–47) – X-rays: stars

---

## 1. Introduction

4U 1630–47 is an X-ray transient that was discovered by *Uhuru* (Jones et al. 1976), with the first recorded outburst in 1969 detected by VELA 5B (Priedhorsky 1986). The first five outbursts were observed by a combination of the VELA 5B, *Uhuru*, OSO 7, and *Ariel V* satellites and seemed to occur every  $\sim 600$  day (Jones et al. 1976; Priedhorsky 1986). The peak

2–10 keV luminosity is  $\sim 2 \times 10^{38}$  erg s<sup>-1</sup> (for an assumed distance of 10 kpc) with the lightcurve often exhibiting a characteristic rapid rise and exponential decay. Typical *e*-folding rise and decay times vary between 1–15 and 20–130 days, respectively (Chen et al. submitted). A strict outburst periodicity was apparently ruled out by an extended 1977 outburst which started  $\sim 70$  days later than predicted and may have lasted for up to six months (Kaluziński et al. 1978; Sims & Watson 1978). In 1984 the source underwent another outburst (Tanaka et al. 1984), the decay of which was observed by EXOSAT (Parmar et al. 1986; hereafter P86). Recently, an archival search revealed the presence of two previously unreported outbursts (Parmar et al. 1995; hereafter P95). The first was observed by the *Einstein* Solid State Spectrometer (SSS) in 1979 and the second by the ROSAT Position Sensitive Proportional Counter (PSPC) in 1992. The times of these outbursts are consistent with the previously reported  $\sim 600$  day outburst recurrence interval, allowing P95 to constrain the recurrence interval to be  $601.7 \pm 3.0$  days. Subsequent ROSAT observations in 1993 did not detect 4U 1630–47 providing stringent upper-limits to any 0.2–2.4 keV quiescent emission (P95).

No bursts or periodicities have been detected from 4U 1630–47 and close to the peak of the 1984 outburst the source exhibited irregular intensity variability with a characteristic timescale of  $\sim 20$  s (P86; Kuulkers et al. 1996b). During this outburst the 1–40 keV EXOSAT spectrum could be modeled by an absorbed soft  $\sim 1$  keV Wien-like component with a high-energy power-law tail. As the outburst decayed, both the low-energy absorption and the relative contribution of the soft component compared to that of the power-law decreased. The *ultra-soft* spectral shape at low energies, the change in relative contributions of the two spectral components, and the lack of detected pulsations or bursts are all indicative of a black hole nature for the compact object. Similar behavior is seen from other X-ray transients such as A 0620–00, GS 1124–684 and GS 2023+338 which are believed to contain black holes on the basis of their dynamically derived masses (e.g. McClintock 1992; Cowley 1994). There are now at least 15 similar black hole X-ray transient (BHXT) systems (White 1994; Tanaka & Lewin 1995) of which five are known to recur (see references in P95). The other BHXT systems have been observed only once

---

Send offprint requests to: A.N. Parmar: aparmar@astro.estec.esa.nl

\* Universities Space Research Association

during the 25 years of satellite observations. This suggests a typical recurrence timescale of 10–50 years. The more prolific outburst activity of 4U 1630–47 is therefore unusual.

We report the results of four *Ginga* and one *ASCA* observation of 4U 1630–47. The *Ginga* observations provide further confirmation of the  $\sim 600$  day period, while the more recent *ASCA* results imply a more complex outburst behavior. In addition, 4U 1630–47 was twice observed by the *Einstein* High Resolution Imager (HRI). During one observation the source was in outburst, while during the second a faint source was detected at a position coincident with 4U 1630–47.

## 2. Observations

### 2.1. *Ginga*

Table 1 lists the *Ginga* Large Area Counter (LAC) observations of 4U 1630–47. The LAC comprised eight multi-wire collimated proportional counters, sensitive in the energy range 1.7–37 keV. Details of the MPC1 and MPC2 data compression modes used in these observations are given in Turner et al. (1989). Background subtraction of *Ginga* LAC data can be performed in a number of ways (Hayashida et al. 1989). One method, often used for sources near the galactic plane, utilizes a nearby off-source measurement obtained just before or after the relevant observation. However, suitable background exposures are not available for any of the observations listed in Table 1. Instead, we estimate the intrinsic background from high galactic latitude source-free observations obtained over three month intervals around the times of observation. Since 4U 1630–47 lies close to the galactic plane ( $l_{\text{II}}, b_{\text{II}} = 336.9^\circ, 0.25^\circ$ ), there is an additional background component due to diffuse X-ray emission (Warwick et al. 1985; Koyama 1989). The shape of this emission is consistent with bremsstrahlung with a narrow emission feature at 6.7 keV superposed (Koyama 1989).

A bremsstrahlung model with variable temperature and normalization together with a narrow emission feature at 6.7 keV was first fit to each of the background subtracted spectra corresponding to the observations listed in Table 1. To avoid complications due to collimator reflection (see below) data below 6.5 keV were excluded from these fits. Similarly, to avoid problems with contamination by a known 22 keV line from the collimator (Turner et al. 1989), data within 2.5 keV of this energy were excluded. In the case of the 1988 April and 1988 October observations this gives satisfactory (at 95% confidence) fits with  $\chi^2$ 's of 40 and 20, respectively, for 28 degrees of freedom (dof). In the case of the 1987 October observation, the fit is unacceptable with a  $\chi^2$  of 54 for 28 dof. Towards the end of the 1984 outburst of 4U 1630–47, when the 1–50 keV luminosity had fallen by a factor  $\sim 300$  from its maximum, the spectrum could be represented by a power-law with a photon index of 1.2 and absorption,  $N_{\text{H}}$ , of  $2 \times 10^{21}$  H atoms  $\text{cm}^{-2}$  (P86). Including such a component in the fits to the 1987 October, and 1988 April and October spectra gives  $\chi^2$ 's of 25, 31, and 19 for 27 dof, respectively. These correspond to values of the F statistic of 35.6, 7.8 and 1.4 implying that this extra component is significant at

$>99\%$  confidence in the first two observations, but not in 1988 October. The  $3\sigma$  confidence upper-limit 1–10 keV luminosity,  $L$ , for an assumed distance of 10 kpc is given in Table 1 for this observation.

This extra emission seen in the 1987 October and 1988 April observations may well originate from 4U 1630–47, but we cannot rule out the possibility of a faint uncatalogued source within the  $1 \times 2^\circ$  full width half maximum field of view (FOV) of the *Ginga* LAC. In particular, an identical analysis to that described above performed on a supposedly source free observation within  $3^\circ$  of 4U 1630–47 on 1988 March 25 gives a value of the F statistic of 13.5, implying the presence of a source at  $>99\%$  confidence. Thus, we conclude that we have a probable detection of 4U 1630–47 in 1987 October, but that the detection in 1988 April may well be spurious.

During the 1989 March observation, when 4U 1630–47 is clearly in outburst, *Ginga* was being operated in an unusual manner. During the two day duration observation, the pointing direction was slowly changed to allow a number of sources on the galactic plane to be scanned. Consequently, the overall exposure to 4U 1630–47 is relatively short and spread over the entire interval. Most of the time, the source was offset in the LAC FOV. This allows scattering of low-energy X-rays off the collimator walls, giving rise to a soft excess (Turner et al. 1989). In order to limit this effect, intervals where the source is viewed with a collimator efficiency of  $<20\%$  were excluded. From a total on-source time of 6678 s, this reduces the exposure to 1334 s, while the mean collimator transmission increases from 0.13 to 0.49. Although it is possible to directly correct the data to remove the soft excess (Williams & Kellett 1991), such a procedure requires a precise knowledge of the satellite pointing direction, which is not available. Therefore, in the spectral fitting discussed below, the presence of this soft excess is accounted for by adding an identical spectral component to the chosen model that is modulated by an exponential cutoff and a variable normalization (Stewart private com.). Thus, if the original spectral model is  $f$ , then the fitted model,  $f'$ , is given by:

$$f' = f + cf \exp\left(\frac{E_{\text{cut}} - E}{E_{\text{fold}}}\right) \quad (1)$$

where  $c$  is the normalization of the scattered component (typically 25% at 1 keV),  $E_{\text{cut}}$  is the cutoff energy (typically 3.5 keV) and  $E_{\text{fold}}$  is the folding energy (typically 0.08 keV). All three parameters are allowed to vary in the fitting process and 0.5% uncertainties were added quadratically to account for calibration uncertainties.

The changing and uncertain pointing direction, the lack of suitable background measurements, the contribution of the diffuse galactic emission and the short exposure time, all combine to limit the quality of the 1989 March *Ginga* spectrum. However, the large collecting area and low intrinsic background of the LAC provides sufficient statistics to justify detailed spectral fitting. Single component power-law, bremsstrahlung, blackbody, cutoff power-law ( $E^{-\Gamma} \exp^{-E/kT}$ ), and multicolor blackbody disk (Mitsuda et al. 1984) models were fit to the spectrum. Each of these models was modified by low-energy absorption using

**Table 1.** *Ginga* observations of 4U 1630–47

| Obs. No. | Start UTC<br>yr mon dy | hr:mn | End UTC<br>yr mon dy | hr:mn | Exp. (s) | Mode | Coll. Trans. | L<br>(erg s <sup>-1</sup> )            | Phase (P95) |
|----------|------------------------|-------|----------------------|-------|----------|------|--------------|--|-------------|
| 1        | 1987 Oct 17            | 05:06 | 1987 Oct 18          | 03:31 | 14656    | MPC1 | 0.45         | $(7.7 \pm_{1.0}^{0.5}) \times 10^{35}$ | 0.12        |
| 2        | 1988 Apr 10            | 12:52 | 1988 Apr 11          | 09:33 | 17183    | MPC2 | 0.37         | $(2.1 \pm_{0.9}^{0.2}) \times 10^{36}$ | 0.41        |
| 3        | 1988 Oct 04            | 23:00 | 1988 Oct 05          | 00:45 | 462      | MPC1 | 0.15         | $< 2.2 \times 10^{36}$                 | 0.71        |
| 4        | 1989 Mar 02            | 20:54 | 1989 Mar 04          | 21:09 | 6678     | MPC2 | 0.13         | $1.1 \times 10^{38}$                   | 0.96        |

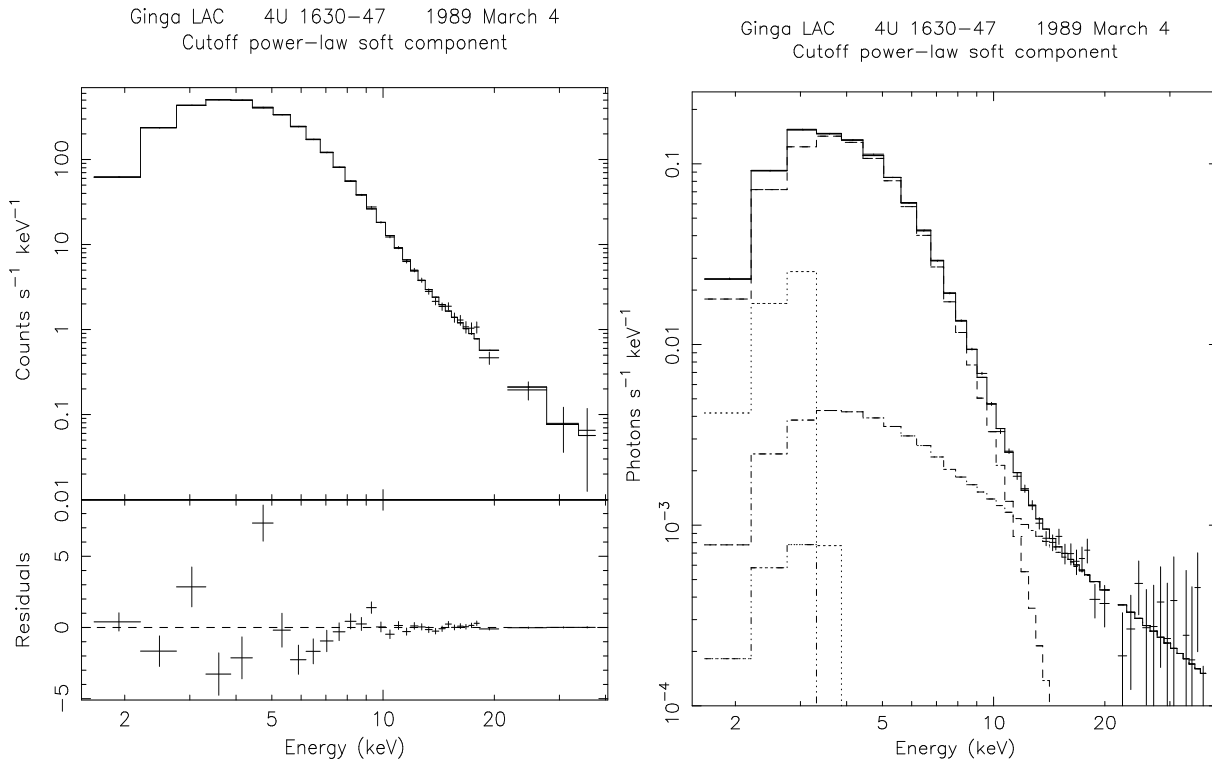


**Fig. 1.** The best-fit cutoff power-law and power-law model modified by collimator scattering shown together with the observed spectrum in the upper left panel. The lower panel shows the residuals. The right panel shows the inferred photon spectrum and the model prediction. The contributions of the two components and from scattering in the collimator (visible below 4 keV) are shown separately

the coefficients of Morisson & McCammon (1983) and the effects of collimator scattering using Eq. (1). The Mitsuda et al. (1984) disk model was chosen to allow comparison with previous BHXT results (e.g. Tanaka & Lewin 1995).

All the above models gave unacceptable fits to the spectrum. The cutoff power-law and multicolor blackbody disk models coming closest to being acceptable, with  $\chi^2_\nu$ 's of  $\sim 15$ . The multicolor disk blackbody model assumes that the gravitational energy released by the accreting material is locally dissipated into blackbody radiation, that the accretion flow is continuous throughout the disk and that the effects of electron scattering on the spectrum are negligible. There are only two parameters in the model;  $R_{\text{in}}(\cos \theta)^{0.5}/d_{10}$  where  $R_{\text{in}}$  is the innermost radius of the disk,  $\theta$  the inclination angle of the disk,  $d_{10}$  the

source distance in units of 10 kpc, and  $T_{\text{in}}$  the blackbody effective temperature at  $R_{\text{in}}$ . If a power-law component of photon index,  $\alpha_{\text{PL}}$ , and normalization,  $a_2$ , is added to these two models, then significantly better fits are obtained with  $\chi^2_\nu$ 's of  $< 2$ . The results of fitting these combined models to the extracted spectrum are presented in Table 2. All spectral uncertainties are given at 68% confidence. Fig. 1 illustrates the best-fit cutoff power-law and power-law model. The best-fit parameters and 1–50 keV luminosity ( $1.2 \times 10^{38}$  erg s<sup>-1</sup>, assuming a distance of 10 kpc) are similar to those obtained by P86 during the first two EXOSAT observations of 4U 1630–47. The best-fit value of  $R_{\text{in}}(\cos \theta)^{0.5}/d_{10}$  is a factor  $\sim 10$  higher than the average of  $\sim 30$  km seen from other BHXT systems (Tanaka & Lewin 1995). This may suggest that the black hole in 4U 1630–47 is

more massive than in these other systems, or it may reflect inadequacies in the spectral modeling. In particular, examination of the residuals in Fig. 1 suggests the presence of an absorption feature at  $\sim 6$  keV, perhaps resulting from a reflection component (e.g. Ebisawa 1991). Including a smeared edge in the spectral model does indeed produce significantly better fits, but is not justified given the uncertainties in background subtraction.

## 2.2. ASCA

The ASCA archive was searched for observations of the region of sky containing 4U 1630-47 and two short observations made on 1994 September 3 between 15:15 and 16:54 UTC and between 16:55 and 18:34 UTC were found. A bright absorbed source, at a position consistent with 4U 1630-47, is visible in both observations in the FOVs of both Gas Imaging Spectrometers (GIS; Tanaka et al. 1994) at offsets of between  $16'$  and  $21'$ . The source is outside the FOV of the SIS detectors in both observations, thus only GIS data were considered. Due to the alignment of the two GIS instruments and the different pointing in the two observations, only data from GIS3 for the first interval and GIS2 for the second interval were analyzed. In each case the source is located  $16'$  off-axis. In the GIS2 first interval and GIS3 second interval, the source is located in regions of high background counting rate and uncertain gain calibration at offset angles of  $21'$ . The standard data selection filters of an Earth elevation angle of  $>5^\circ$ , and a cutoff rigidity of  $>6$  GeV  $c^{-1}$  were applied. This gives a total exposure of 1600 s for the first interval and 1880 s for the second. The spectra were extracted using events accumulated within  $10'$  radii centered on the source positions and the backgrounds estimated from identically sized regions located diametrically opposite in the FOVs. The mirror vignetting correction was applied giving a count rate of  $13$   $s^{-1}$ , during both observations. For spectral fitting, the response matrices “gis2v4\_0” and “gis3v4\_0” (1995 March 2) provided by the ASCA Guest Investigator Facility and corrected for vignetting were used. The spectra were rebinned to have at least 20 photons in each channel and simultaneously fit.

The same spectral models as applied to the *Ginga* data were used, except that a high-energy power-law component is not necessary due to the limited energy response of the GIS, which results in few detected counts above 8 keV. Both the cutoff power-law and the multicolor blackbody disk models gave satisfactory fits with similar values of  $\chi^2_\nu$  of  $\sim 1$ . The best-fit parameters are listed in Table 3 and are significantly different from those derived by *Ginga*. Fig. 2 shows the best-fit multicolor blackbody disk model fit to the GIS spectra. The best-fit parameters for both models give a 1–50 keV luminosity of  $(2.0\text{--}2.4) \times 10^{37}$  erg  $s^{-1}$ . This is a factor 4 lower than during the second EXOSAT observation (P86), which occurred 40 days after the outburst start (P95). The spectral parameters given in P86 for the cutoff power-law model for the second EXOSAT observation are different from the best-fit values derived here using ASCA. However, if  $\Gamma$  is fixed at a value of  $-2$ , consistent with the EXOSAT observations, the fit to the ASCA spectra still

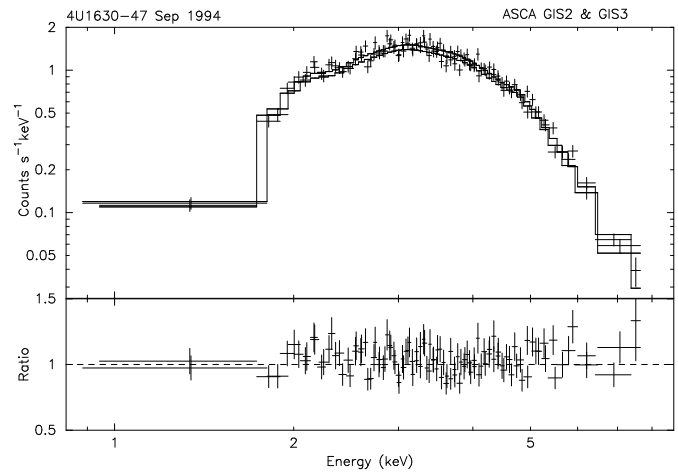


**Fig. 2.** The best-fit multicolor blackbody disk shown together with the observed GIS2 and GIS3 spectra in the upper panel. The lower panel shows the ratio of model to the data

gives an acceptable  $\chi^2$  of 499 for 511 dof. The best-fit temperature is now  $0.78 \pm 0.02$  keV, comparable with that during the second EXOSAT observation. The 90% confidence upper-limit to a narrow emission line at 6.4 keV is 55 eV.

## 2.3. Einstein

4U 1630-47 was observed by the *Einstein* HRI (Giacconi et al. 1979) on 1979 February 22 between 21:17 and 23:04 UTC for an exposure of 4132 s and on 1980 February 18 between 17:49 and 18:26 UTC for an exposure of 2007 s. During the 1979 observation, which occurred 13 days before the *Einstein* SSS observation reported in P95, a source was detected at a location consistent with 4U 1630-47 with a count rate of  $0.409 \pm 0.011$   $s^{-1}$ . (All quoted HRI count rates are corrected for instrument sampling deadtime losses, mirror vignetting, and for events that fall outside the extraction region). The high HRI count rate means that 4U 1630-47 was clearly in outburst during the observation, consistent with the ephemeris in P95 and the SSS detection 13 days later. The position is R.A. =  $16^h 34^m 01.3^s$ ,  $\delta = -47^\circ 23' 34.3''$  (J2000) which is  $10''$  from the center of the 90% confidence  $10''$  radius EXOSAT position for 4U 1630-47 in P86.

During the 1980 HRI observation, which occurred at an outburst ephemeris of 0.48 (i.e. approximately mid-way between expected outburst times), a faint source was detected at a position consistent with 4U 1630-47 with a count rate of  $0.0078 \pm 0.0023$   $s^{-1}$ . Source counts were extracted from a circular region centered on the source with a radius of  $10''$ . The background rates were extracted from a concentric annular region with inner and outer radii of  $32''$  and  $60''$ , respectively. The extraction radii were chosen to optimize the signal to noise ratio. The total number of counts detected was 15 with an expected background of 1.38 counts. The probability that the source arises from a fluctuation in the background counting rate is  $3 \times 10^{-11}$ , assuming Poisson statistics.

**Table 2.** Fit results to the 1989 March *Ginga* spectrum

| Model                                     | Disk blackbody<br>+ power-law    | Cutoff power-law<br>+ power-law  | Units                                  |
|---|----------------------------------|----------------------------------|--|
| $T_{\text{in}}$                           | $1.233 \pm 0.003$                |                                  | keV                                    |
| $R_{\text{in}}(\cos \theta)^{0.5}/d_{10}$ | $306.9 \pm 1.1$                  |                                  | km                                     |
| $\Gamma$                                  |                                  | $-1.43 \pm 0.07$                 |  |
| kT  |                                  | $1.071 \pm 0.015$                | keV                                    |
| $\alpha_{\text{PL}}$                      | $1.01^{+0.02}_{-0.01}$           | $1.74^{+0.19}_{-0.01}$           |  |
| $a_2$                                     | $(9.76 \pm 0.46) \times 10^{-3}$ | $(8.10 \pm 0.20) \times 10^{-2}$ | photons $\text{cm}^{-2} \text{s}^{-1}$ |
| $N_{\text{H}}$                            | $9.51 \pm 0.11$                  | $7.75 \pm 0.18$                  | $10^{22}$ H atoms $\text{cm}^{-2}$     |
| $\chi^2_{\nu}$                            | 1.83 for 36 dof                  | 1.52 for 35 dof                  |  |

**Table 3.** Fit results to the ASCA GIS spectra<sup>a</sup>

| Model                                     | Disk blackbody   | Cutoff power-law | Units                              |
|---|------------------|------------------|------------------------------------|
| $T_{\text{in}}$                           | $0.98 \pm 0.02$  |                  | keV                                |
| $R_{\text{in}}(\cos \theta)^{0.5}/d_{10}$ | $127 \pm 20$     |                  | km                                 |
| $\Gamma$                                  |                  | $-0.35 \pm 0.80$ |                                    |
| kT  |                  | $1.2 \pm 0.4$    | keV                                |
| $N_{\text{H}}$                            | $6.4 \pm 0.2$    | $6.8 \pm 0.8$    | $10^{22}$ H atoms $\text{cm}^{-2}$ |
| $\chi^2_{\nu}$                            | 0.94 for 511 dof | 0.94 for 510 dof |                                    |

### 3. The outburst ephemeris

Table 4 lists the known outbursts from 4U 1630–47 and is an updated version of that in P95. The derivation of the outburst times, except those for cycles 11, 12, 15, and 16 are reported in P95. Outburst 16 was observed by both the All Sky Monitor (ASM) and Proportional Counter Array instruments on the *Rossini* X-ray Timing Explorer (XTE). The ASM intensity of 4U 1630–47 increased from  $<20$  mCrab to about 200 mCrab on around 1996 March 20 and remained steady at this level until at least 1996 May 1 (Levine et al. 1996; Marshall 1996). We therefore assume an outburst start time of 1996 March 20 with an uncertainty of  $\pm 10$  days. Since the observations presented here only provide brief snapshots of the outbursts, it is necessary to estimate the outburst phases at which they occurred so that the times of maxima can be derived.

The TTM instrument on the *Mir* Space Station observed 4U 1630–47 in outburst on 1989 March 24–25 (in 't Zand 1992). Using the best-fitting thermal bremsstrahlung spectrum of in 't Zand (1992) of  $kT=2.5 \pm 0.2$  keV and absorption of  $(1.0 \pm 0.3) \times 10^{23}$  H atoms  $\text{cm}^{-2}$  gives a 2–28 keV intensity of  $5.2 \times 10^{-9}$  erg  $\text{cm}^{-2} \text{s}^{-1}$ . This is  $\sim 30\%$  higher than the intensity observed by *Ginga* 22 days earlier of  $4.0 \times 10^{-9}$  erg  $\text{cm}^{-2} \text{s}^{-1}$  and suggests that the *Ginga* observation may have occurred during the rising phase of the outburst. We therefore assume that outburst maximum occurred mid-way between the TTM and *Ginga* observations. Since the other out-

bursts have a typical  $e$ -folding time of 50 days, we have made a conservative estimate for the uncertainty in outburst maximum of  $\pm 25$  days (Table 4).

If the excess emission observed by *Ginga* during the 1987 October observation originates from 4U 1630–47, we can use the known outburst properties to estimate the time of outburst maximum. Since the luminosity and power-law spectral shape are similar to those during the final EXOSAT observation reported in P86 which occurred  $\sim 120$  days after the start of the 1984 outburst, we have made a conservative estimate for the 1987 outburst start time by subtracting 120 days from the time of observation. We assign an uncertainty of  $\pm 50$  days to the outburst start time derived in this way (Table 4).

The 1–50 keV luminosity observed by ASCA in 1994 September is a factor 4 less than observed during the second EXOSAT observation of 4U 1630–47 reported in P86. However, as discussed in Sect. 2.2, the spectral shapes are similar. This suggests that the ASCA observation took place at a similar, or later, outburst phase than the second EXOSAT observation which occurred 40 days after the start of the 1984 outburst (P95). The difference in luminosities and an  $e$ -folding time of 50 days suggests that the ASCA observation may have occurred up to 70 days later in the outburst than the second EXOSAT observation. We therefore assume that the ASCA observation took place midway between these two extremes and subtract 75 days from the observation time to derive the outburst start time (Table 4).

**Table 4.** 4U 1630–47 outburst observations

| Cycle | Year | Outburst Peak Date (MJD) | O–C (days) | Comment               | Satellite                     | Reference |
|-------|------|--------------------------|------------|-----------------------|-------------------------------|-----------|
| 0     | 1969 | 40396 ± 15               | 28.0       | Most of outburst      | VELA 5B                       | 1         |
| 1     | 1971 | 41005 ± 15               | 26.9       | Entire outburst       | VELA 5B, <i>Uhuru</i>         | 1,2       |
| 2     | 1972 | 41589 ± 15               | 0.9        | Entire outburst       | VELA 5B, <i>Uhuru</i> , OSO 7 | 1,2,3     |
| 3     | 1974 | 42167 ± 15               | −31.1      | Entire outburst       | VELA 5B, <i>Uhuru</i>         | 1,2       |
| 4     | 1976 | 42795 ± 15               | −13.2      | Entire outburst       | VELA 5B, <i>Ariel V</i>       | 1,2       |
| 5     | 1977 | 43468 ± 15               | 49.8       | Entire outburst       | <i>Ariel V</i> , HEAO-1       | 4,5,6     |
| 6     | 1979 | 43902 ± 40               | −126.3     | Two observations      | <i>Einstein</i>               | 7         |
| 9     | 1984 | 45791 ± 15               | −67.4      | Short observations    | <i>Tenma</i> , EXOSAT         | 8,9       |
| 11    | 1987 | 46966 ± 50               | −112.5     | Single observation    | <i>Ginga</i>                  | 10        |
| 12    | 1989 | 47598 ± 25               | −90.5      | Two observations      | <i>Mir</i> -TTM, <i>Ginga</i> | 10,11     |
| 14    | 1992 | 48845 ± 40               | −63.6      | Single observation    | ROSAT                         | 7         |
| 15    | 1994 | 49523 ± 50               | 4.4        | Single observation    | ASCA                          | 10        |
| 16    | 1996 | 50162 ± 10               | 33.3       | Multiple observations | XTE                           | 12,13     |

<sup>1</sup>Priedhorsky (1986); <sup>2</sup>Jones et al. (1976); <sup>3</sup>Markert et al. (1979); <sup>4</sup>Kaluzienski & Holt (1977); <sup>5</sup>Kaluzienski et al. (1978); <sup>6</sup>Sims & Watson (1978); <sup>7</sup>P95; <sup>8</sup>Tanaka et al. (1984); <sup>9</sup>P86; <sup>10</sup>This paper; <sup>11</sup>in 't Zand (1992); <sup>12</sup>Marshall (1996); <sup>13</sup>Levine et al. (1996).

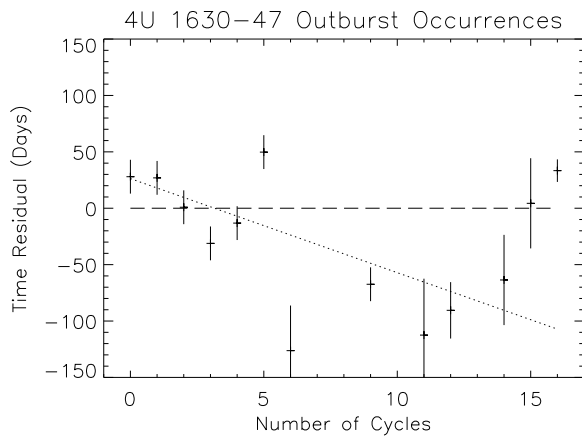


**Fig. 3.** The time residual in days after a linear fit of the outburst times to cycle number. The error bars reflect the uncertainties in deriving the outburst start times (see text). The dotted line shows the best-fit ephemeris of P95 which excludes the cycle 11, 12, 15, and 16 measurements

We assign an uncertainty of  $\pm 40$  days to the outburst start time derived in this way.

Inspection of the outburst times derived above reveals that the *Ginga* outburst times are in agreement with the ephemeris given in P95, but that the ASCA and XTE outburst times are 100–150 days late. Similar behavior has been noted before. The 1977 outburst occurred 50–70 days late (Kaluzienski & Holt 1977), and may have lasted for up to six months (Kaluzienski et al. 1978; Sims & Watson 1978). The subsequent outburst was observed by *Einstein* and appeared to start  $\sim 120$  days early (Table 4). This implies, that at times, 4U 1630–47 can undergo more complex outburst behavior. A linear fit to all the outburst

times listed in Table 4 gives an unacceptable fit with a  $\chi^2$  of 85 for 11 dof. The mean outburst recurrence interval is 610.0 day, and the outburst epoch of JD 2,440,368.5. These values are inconsistent with the ephemeris reported in P95. The average deviation of the outburst times from this linear relation is  $\pm 49$  day (Fig. 3). If the last two outbursts are ignored then the ephemeris is consistent with that of P95 which is shown as a dotted line in Fig. 3. This sort of behavior is reminiscent of the superoutbursts observed from SU UMa stars. In these systems, the superoutbursts follow a linear ephemeris for 10–20 cycles, with a standard deviation of only 5–10% of the corresponding period. Occasionally, the mean cycle length switches to one of another 2–3 period values which are characteristic of each star (e.g. Vogt 1980). Observations of subsequent outbursts from 4U 1630–47 will reveal whether the recent anomalous behavior continues, or whether the timing reverts to that predicted by the ephemeris in P95.

#### 4. Transient behavior

4U 1630–47 has the shortest outburst recurrence interval of any known BHXT. The large number of observed outbursts provides a unique data set by which to study the BHXT outburst mechanism. The nature of these outbursts is still uncertain (see e.g. Lasota 1996), although recently an accretion disk instability trigger has been favored above the mass transfer instability model (see Narayan et al. 1996; van Paradijs 1996). Van Paradijs & Verbunt (1984) proposed that outbursts in low-mass X-ray binaries and dwarf novae may have a similar origin. Based on the similarity between the recurrence intervals of SU UMa outbursts and the timescales of the quasi-periodic intensity cycles seen from a number of persistent low-mass X-ray binaries, Priedhorsky (1986) and Priedhorsky & Holt (1987) suggested

**Table 5.** Candidate BHXT quiescent X-ray emission

| Source       | Quiescent<br>luminosity<br>( $\text{erg s}^{-1}$ )          | d<br>(kpc) | Reference                |
|--------------|---|------------|--------------------------|
| GRO J0422+32 | $<2 \times 10^{32}$   | 2          | Callanan et al. (1996)   |
| A 0620-00    | $6 \times 10^{30}$  | 1          | McClintock et al. (1995) |
| GS 1124-684  | $<6 \times 10^{32}$   | 11         | Greiner et al. (1994a)   |
| A 1524-617   | $<1 \times 10^{34}$   | 4.4        | Barret et al. (1995)     |
| 4U 1543-47   | $<3 \times 10^{32}$   | 4          | Greiner et al. (1994b)   |
| 4U 1630-47   | $<7 \times 10^{32}/d_{10}^2$<br>$8 \times 10^{33}/d_{10}^2$ | 10         | This paper<br>This paper |
| GRO J1655-40 | $<3 \times 10^{32}$   | 3          | Greiner et al. (1995)    |
| H 1705-250   | $<5 \times 10^{32}$   | 3          | Verbunt et al. (1994)    |
| GRS 1915+105 | $<3 \times 10^{35}$   | 12.5       | Greiner et al. (1994c)   |
| GS 2000+251  | $<1 \times 10^{31}$   | 2          | Verbunt et al. (1994)    |
| GS 2023+338  | $8 \times 10^{33}$  | 3.5        | Wagner et al. (1994)     |

that these two types of systems are more suited to comparative studies. SU UMa systems often show superoutbursts in addition to normal outbursts (see e.g. Warner 1995). These outbursts are stronger and have longer durations and recurrence times than the normal ones. During superoutbursts optical variations with periods slightly longer than the orbital period may be observed (superhumps). The detection of superhumps during some BHXT outbursts has strengthened this similarity (Charles et al. 1991; Bailyn 1992; Kato et al. 1995). A further similarity between BHXTs and SU UMa systems was proposed by Kuulkers et al. (1996a) who noticed that some extreme members of the SU UMa class, the “tremendous outburst amplitude dwarf novae”, or TOADs, have the following characteristics very similar to those of BHXTs: (a) long quiescent intervals between large-amplitude outbursts; (b) no intervening normal outbursts; (c) optical outburst lightcurves exhibiting both “glitches” and superhumps; (d) very small mass ratios; and (e) very low mass transfer rates during quiescence (Kuulkers et al. 1996a, and references therein). The similarity in properties may indicate that the underlying mechanism which produces TOAD and BHXT outbursts is the same.

The 4U 1630-47 outburst recurrence interval of 1.6 yrs is shorter than those of other BHXTs of 10-50 yrs and those of typical TOADs, which have recurrence times of up to decades. The 4U 1630-47 outburst recurrence interval is more similar to those of the superoutbursts of the shorter recurrence outbursting TOADs, such as SW UMa ( $\sim 1-4$  years; Howell et al. 1995). Interestingly, the superoutburst recurrence intervals of individual SU UMa sources vary by  $\lesssim 10\%$  (Vogt 1980), which is similar to the variation in the 4U 1630-47 outburst times of  $\sim 8\%$ .

## 5. Quiescent emission

The properties of BHXTs in quiescence are important in understanding the physics of accretion onto compact objects at an

extremely low mass flow rate, and for understanding the mechanism of the transient X-ray outbursts. McClintock et al. (1995) detected A 0620-00, 16 years after its 1975 outburst using the ROSAT PSPC. The intensity of  $0.0013 \pm 0.0003$  counts  $\text{s}^{-1}$  corresponds to a luminosity of  $6 \times 10^{30}$  erg  $\text{s}^{-1}$  for a distance of 1 kpc, a blackbody temperature of 0.16 keV and an assumed absorption of  $1.2 \times 10^{21}$  H atoms  $\text{cm}^{-2}$ . This spectrum predicts  $2.5 \times 10^{-4}$  counts  $\text{s}^{-1}$  in the *Einstein* HRI, a factor  $\sim 30$  less than observed from 4U 1630-47. GS 2023+338 (V404 Cyg) was detected 3.5 years after its 1989 outburst by Wagner et al. (1994) using the ROSAT PSPC. The average count rate of  $0.024 \pm 0.001$   $\text{s}^{-1}$  corresponds to a luminosity of  $8 \times 10^{33}$  erg  $\text{s}^{-1}$  for a likely distance of 3.5 kpc. The source exhibited factor 10 intensity variability during quiescence on a timescale of less than half a day. The mean spectrum can be represented by a blackbody with temperature 0.21 keV and absorption of  $1.5 \times 10^{22}$  H atoms  $\text{cm}^{-2}$ . This spectrum predicts  $2.1 \times 10^{-3}$  counts  $\text{s}^{-1}$  in the *Einstein* HRI, a factor  $\sim 4$  less than observed from 4U 1630-47. Upper-limits to the quiescent 0.2-2.4 keV luminosity from other BHXTs are given in Table 5. For 4U 1543-47, a 0.2 keV blackbody spectrum with absorption of  $3.1 \times 10^{21}$  H atoms  $\text{cm}^{-2}$  is assumed in order to convert the upper limit count rate in Greiner et al. (1994b) to a luminosity.

It is notable that both BHXTs previously detected in quiescence have soft spectra consistent with blackbodies with temperatures of  $\sim 0.2$  keV. If this spectral shape is assumed, together with absorption of  $2 \times 10^{21}$  H atoms  $\text{cm}^{-2}$  as observed by P86 towards the end of the 1984 outburst, then it is possible to estimate the quiescent luminosity of 4U 1630-47 for a given distance. Since the distance to 4U 1630-47 is poorly constrained we assume 10 kpc, as adopted by P86 and Chen et al. (submitted). At this distance, the 0.2-2.4 keV luminosity at the time of the *Einstein* HRI detection is  $7.8 \times 10^{33}$  erg  $\text{s}^{-1}$ , while the ROSAT PSPC upper limit obtained by combining the two non-detections in P95 corresponds to a 0.2-2.4 keV luminosity of  $6.7 \times 10^{32}$  erg  $\text{s}^{-1}$ . It is unclear whether the X-rays detected during the *Einstein* HRI observation are from “true” quiescent emission i.e., they result from the mass transfer necessary to provide sufficient accumulated material for the next outburst, or whether the 1979 outburst was anomalously long. Alternatively, the emission may originate from a previously undetected type of low-level inter-outburst activity.

*Acknowledgements.* This research has made use of data obtained from the Leicester Database and Archive Service at the Department of Physics and Astronomy, Leicester University, UK and from the High Energy Astrophysics Science Archive Research Center, provided by the NASA-Goddard Space Flight Center. E. Kuulkers acknowledges an ESA Research Fellowship. We thank J. Grindlay for pointing out the existence of the *Einstein* HRI observations.

## References

- Bailyn C.D., 1992, ApJ 391, 298  
 Barret D., Motch C., Pietsch W., Voges W., 1995, A&A 296, 459  
 Callanan P.J., Garcia M.R., McClintock J.E., et al., 1996, ApJ 461, 351  
 Charles P.A., Kidger M.R., Pavlenko E.P., et al., 1991, MNRAS 249, 567

- Cowley A.P., 1994, AIP Conf. Proc. 308, 45  
 Ebisawa K., 1991, PhD Thesis, ISAS, Japan  
 Giacconi R., Branduardi G., Briel U., et al., 1979, ApJ 230, 540  
 Greiner J., Hasinger G., Molendi S., Ebisawa K., 1994a, A&A 285, 509  
 Greiner J., Predehl P., Harmon B.A., 1994b, AIP Conf. Proc. 304, 314  
 Greiner J., Snowden S., Harmon, B.A., Kouveliotou C., Paciesas W., 1994c, AIP Conf. Proc. 304, 260  
 Greiner J., Predehl P., Pohl M., 1995, A&A 297, L67  
 Hayashida K., Inoue H., Koyama, K., et al., 1989, PASJ 41, 373  
 Howell S.B., Szkody P., Sonneborn G., et al., 1995, ApJ 453, 454  
 In 't Zand J., 1992, PhD Thesis, SRON, Utrecht  
 Jones C., Forman W., Tananbaum H., Turner M.J.L., 1976, ApJ 210, L9  
 Kaluzienski L.J., Boldt E.A., Holt S.S., Mushotzky R.F., et al., 1978, IAU Circ. 3197  
 Kaluzienski L.J., Holt S.S., 1977, IAU Circ. 3144  
 Kato T., Mineshige S., Hirata R., 1995, PASJ 47, 31  
 Koyama K., 1989, PASJ 41, 665  
 Kuulkers E., Howell S.B., van Paradijs J., 1996a, ApJ 462, L87  
 Kuulkers E., van der Klis M., Parmar A.N., 1996b, ApJ, submitted  
 Lasota J.P., 1996, Mechanisms for dwarf nova outbursts and soft X-ray transients. In: van Paradijs, J., van den Heuvel E.P.J., Kuulkers E. (eds.) Compact Stars in Binaries, Proc. IAU Symp. 165. Kluwer, Dordrecht, p. 43  
 Levine A.H., Bradt H., Chakrabarty D., et al., 1996, IAU Circ. 6390  
 Markert T.H., Winkler P.F., Laird F.N., et al., 1979, ApJS 39, 573  
 Marshall F.E., 1996, IAU Circ. 6389  
 McClintock J.E., 1992, NATO ASI Series C 377, 27  
 McClintock J.E., Horne K., Remillard R.A., 1995, ApJ 442, 365  
 Mitsuda K., Inoue H., Koyama K., et al., 1984, PASJ 36, 741  
 Morisson D., McCammon D., 1983, ApJ 270, 119  
 Narayan R., McClintock J.E., Yi I., 1996, ApJ 457, 821  
 Parmar A.N., Stella L., White N.E., 1986, ApJ 304, 664 (P86)  
 Parmar A.N., Angelini L., White N.E., 1995, ApJ 452, L129 (P95)  
 Priedhorsky W.C., 1986, Astrophys. Space Sci. 126, 89  
 Priedhorsky W.C., Holt S.S., 1987, Space Sci. Rev. 45, 291  
 Sims M.R., Watson M.G., 1978, IAU Circ. 3227  
 Stewart G.C., 1991, private communication  
 Tanaka K., and the *Tenma* team, 1984, IAU Circ. 3936  
 Tanaka K., Holt S.S., Inoue H., 1994, PASJ 46, L37  
 Tanaka K., Lewin W.H.G., 1995, Black-hole binaries. In: Lewin W.H.G., van Paradijs J., van den Heuvel E.P.J. (eds.) X-ray Binaries. Cambridge Univ. Press, Cambridge, p. 121  
 Turner M.J.L., Thomas H.D., Patchett B.E., Reading D.H., Makishima K., 1989, PASJ 41, 345  
 Van Paradijs J., 1996, ApJ 464, L139  
 Van Paradijs J., Verbunt F. 1984, AIP Conf. Proc. 115, 49  
 Verbunt F., Belloni T., Johnston H.M., van der Klis M., Lewin W.H.G., 1994, A&A, 285, 903  
 Vogt N., 1980, A&A 88, 66  
 Wagner R.M., Starrfield S.G., Hjellming R.M., Howell S.B., Kreidl T.J., 1994, ApJ 429, L25  
 Warwick R.S., Turner M.J.L., Watson M.G., Willingale R., 1985, Nature 317, 218  
 Warner B., 1995, Cataclysmic Variable Stars. Cambridge Univ. Press, Cambridge  
 White N.E., 1994, AIP Conf. Proc. 308, 53  
 Williams O.R., Kellett B.J., 1991, An Introduction to Ginga Data Reduction, University of Leicester Starlink Local User Note 17.1

This article was processed by the author using Springer-Verlag L<sup>A</sup>T<sub>E</sub>X A&A style file L-AA version 3.